Cell Reports
Article

The lncRNA *Malat1* Is Dispensable for Mouse Development but Its Transcription Plays a *cis*-Regulatory Role in the Adult

Bin Zhang,[1] Gayatri Arun,[1] Yuntao S. Mao,[1,6] Zsolt Lazar,[1] Gene Hung,[2] Gourab Bhattacharjee,[2] Xiaokun Xiao,[2] Carmen J. Booth,[3] Jie Wu,[1,4] Chaolin Zhang,[5] and David L. Spector[1,*]
[1]Cold Spring Harbor Laboratory, One Bungtown Road, Cold Spring Harbor, NY 11724, USA
[2]Isis Pharmaceuticals, 2855 Gazelle Court, Carlsbad, CA 92010, USA
[3]Section of Comparative Medicine, Yale University School of Medicine New Haven, CT 06520, USA
[4]Department of Applied Mathematics and Statistics, Stony Brook University, Stony Brook, NY 11794, USA
[5]Laboratory of Molecular Neuro-Oncology, Howard Hughes Medical Institute, The Rockefeller University, New York, NY 10021, USA
[6]Present address: Department of Chemistry and Chemical Biology, Harvard University, Cambridge, MA 02138, USA
*Correspondence: spector@cshl.edu
http://dx.doi.org/10.1016/j.celrep.2012.06.003

SUMMARY

Genome-wide studies have identified thousands of long noncoding RNAs (lncRNAs) lacking protein-coding capacity. However, most lncRNAs are expressed at a very low level, and in most cases there is no genetic evidence to support their in vivo function. *Malat1* (metastasis associated lung adenocarcinoma transcript 1) is among the most abundant and highly conserved lncRNAs, and it exhibits an uncommon 3′-end processing mechanism. In addition, its specific nuclear localization, developmental regulation, and dysregulation in cancer are suggestive of it having a critical biological function. We have characterized a *Malat1* loss-of-function genetic model that indicates that *Malat1* is not essential for mouse pre- and postnatal development. Furthermore, depletion of *Malat1* does not affect global gene expression, splicing factor level and phosphorylation status, or alternative pre-mRNA splicing. However, among a small number of genes that were dysregulated in adult *Malat1* knockout mice, many were *Malat1* neighboring genes, thus indicating a potential *cis*-regulatory role of *Malat1* gene transcription.

INTRODUCTION

Recent genome-wide studies have indicated that the majority of the human and mouse genomes are transcribed, yielding a complex network of transcripts that includes thousands of noncoding RNAs (ncRNAs) with no protein-coding capacity (Chodroff et al., 2010; Guttman et al., 2009; reviewed in Kapranov et al., 2007; Ørom et al., 2010). Long noncoding RNAs (lncRNAs), the largest and most complex class of ncRNAs, are mRNA-like RNA polymerase II transcripts ranging in size from 200 nt to >100 knt, and many exhibit cell-type-specific expression (Chodroff et al., 2010; Guttman et al., 2009; Orom et al., 2010). The majority of lncRNAs are expressed at very low levels, some as low as one or less than one copy per cell (Mercer et al., 2012), and these RNAs generally exhibit poor primary sequence conservation over evolution. LncRNAs have been implicated in numerous molecular functions, including modulating transcriptional patterns, regulating protein activities, serving structural or organizational roles, altering RNA processing events, and serving as precursors to small RNAs (reviewed in Wilusz et al., 2009). However, most of these molecular functions were deduced from studies performed in cell lines upon lncRNA overexpression or knockdown. Except for a few examples, such as *Xist* involved in X chromosome inactivation (Marahrens et al., 1997) and *Kcnq1ot1* (Mohammad et al., 2010) and *Air* (Sleutels et al., 2002) in genomic imprinting, genetic evidence supporting the in vivo function of most mammalian lncRNAs is lacking.

The lncRNA *HOTAIR* has recently been studied in knockdown cell lines and shown to regulate expression of *HoxD* genes in *trans* by associating with chromatin modification complexes such as PRC2, LSD1, and CoREST/REST (Khalil et al., 2009; Rinn et al., 2007; Tsai et al., 2010) and to be overexpressed in breast cancer and regulate metastasis by reprogramming chromatin via polycomb complexes (Gupta et al., 2010). Interestingly, genetic deletion of the mouse *HoxC* cluster containing the *Hotair* gene did not result in misregulation of *HoxD* genes or any phenotype at the molecular or organismal level (Schorderet and Duboule, 2011). Noncoding nuclear-enriched abundant transcript 1 (*Neat1,* a.k.a. *Men ε/β)* lncRNA has been shown to be essential for the assembly and maintenance of nuclear paraspeckles (Clemson et al., 2009; Mao et al., 2011; Sasaki et al., 2009; Sunwoo et al., 2009) and nuclear retention of some hyperedited RNAs in hESCs and HeLa cells (Chen and Carmichael, 2009). Surprisingly, a study of *Neat1* hypomorphic mouse mutants, although lacking paraspeckles, failed to exhibit any physiological defects (Nakagawa et al., 2011). While these lncRNAs do not appear to be essential during pre- or postnatal mouse development, their regulatory function may be masked by redundant or compensatory mechanisms and may only be revealed upon specific stress conditions, which have thus far not been investigated. Interestingly, a recent study in zebrafish

identified 29 evolutionarily conserved lncRNAs, and of these, two exhibited a significant regulatory function during zebrafish development, as demonstrated by morpholino intervention (Ulitsky et al., 2011). Further in vivo analyses of lncRNAs are necessary to reveal their mechanisms of action.

Malat1 (metastasis associated lung adenocarcinoma transcript 1), also known as *Neat2* (noncoding nuclear-enriched abundant transcript 2), is located on mouse chromosome 19qA (human chromosome 11q13.1). *Malat1* is evolutionarily conserved among mammals in terms of its primary sequence, and it is highly expressed in many tissues and regulated during tissue differentiation (Bernard et al., 2010; Hutchinson et al., 2007; Ji et al., 2003). *MALAT1* is also upregulated in several human cancers, suggesting that it may have an important function during cancer progression (Guffanti et al., 2009; Ji et al., 2003). Knockdown of *MALAT1* by antisense oligonucleotides (ASOs) has been shown to affect the recruitment of pre-mRNA splicing factors to a reporter locus in human U2OS cells and to alter synapse number in cultured neurons (Bernard et al., 2010). Recently, *MALAT1* depletion in HeLa cells was shown to perturb the protein level and phosphorylation status of two pre-mRNA splicing factors and the pre-mRNA splicing pattern of a set of transcripts (Tripathi et al., 2010). In addition, a large fraction of cells accumulated at the G2/M boundary and an increased cell death was observed (Tripathi et al., 2010). In contrast, a second study examining the effect of knockdown of *MALAT1* in HeLa cells observed a loss of serum-induced cell proliferation and E2F1 target gene expression with profound G1/S arrest, but no apparent G2/M arrest or cell death (Yang et al., 2011). *MALAT1* was shown to be part of a complex that binds to unmethylated Pc2 at nuclear speckles promoting E2F1 SUMOylation, leading to activation of the growth-control gene program (Yang et al., 2011). However, the physiological function of *Malat1* lncRNA at the tissue and organismal levels has not been investigated.

Here, we show that *Malat1* is one of the most abundant lncRNAs in mouse liver and brain cortex. To assess the potential in vivo function of mouse *Malat1*, we first evaluated the consequences of its knockdown in adult mice by using an antisense approach and found no significant morphologic change in tissue organization upon its transient depletion. The *Malat1* locus is syntenically conserved from fish to human, and its high transcription rate is also maintained through evolution despite limited sequence conservation, suggesting that transcription of the *Malat1* gene per se may carry a biological function. To examine the role of the *Malat1* gene locus, we also established a mouse loss-of-function genetic model. Detailed whole-body histopathologic characterization showed that *Malat1* ncRNA and its transcription are dispensable for mouse pre- and postnatal development. Further cell biological and biochemical analyses indicated that *Malat1* lncRNA is not essential for nuclear speckle assembly/maintenance, the level and phosphorylation status of serine/arginine-rich (SR) splicing factors, or cell proliferation and viability. Genome-wide expression and splicing profiling of mouse liver and brain cortex demonstrated that *Malat1* loss results in minimal alterations in global gene expression and pre-mRNA splicing. However, inactivation of the *Malat1* gene results in a nearly 2-fold upregulation of several genes that reside adjacent to the *Malat1* locus, including the lncRNA *Neat1*. These results suggest a model whereby transcription by the highly active *Malat1* promoter may be important for regulating the expression of nearby genes in *cis*.

RESULTS

Malat1 Encodes a Highly Abundant lncRNA in Mouse

To assess the level of *Malat1* lncRNA in mouse, we performed RNA-seq profiling and obtained ~230 and ~220 million paired-end reads from three wild-type mouse livers and three brain cortices, respectively. We first focused on profiles of ~1,700 lncRNA genes in RefSeq (see Experimental Procedures). Consistent with previous findings, we found that most lncRNA genes are expressed at lower levels as compared to protein-coding genes (Figures 1A and 1B). However, the fragments per kilobase million reads (FPKM) value for *Malat1* is comparable or higher than several housekeeping protein-coding genes (in liver: *Malat1*, 109 FPKM; *Actb*, 177 FPKM; *Gapdh*, 21 FPKM; in brain cortex: *Malat1*, 199 FPKM; *Actb*, 484 FPKM; *Gapdh*, 16 FPKM). *Malat1* is highly expressed in both brain cortex and liver (Figures 1A–1C and Table S1) and comprises ~15.2% of total lncRNA sequence reads in liver and ~5.7% in brain cortex.

Interestingly, the *Malat1* gene resides adjacent to *Neat1*, another lncRNA gene on mouse Chr.19 (Figure 1D). The nuclear-retained *Malat1* ncRNA is ~6.7 knt (kilonucleotide) and the nuclear retained *Neat1* RNA exists as two isoforms of 3.2 knt (*Neat1_1*) and ~20 knt (*Neat1_2*) (Sunwoo et al., 2009) (Figure 1D). Conservation analysis showed that both *Malat1* and *Neat1_1* are among the most conserved lncRNAs during vertebrate evolution (data not shown) with minimal repetitive elements (Figure 1D). Similar to *Malat1*, *Neat1* is also highly and widely expressed in adult tissues (Figures 1A–1C) (Hutchinson et al., 2007). A recent study has shown that both RNA molecules have a unique 3′ end processing module, which is conserved from fish to human (Figure 1D) (Sunwoo et al., 2009; Wilusz et al., 2008). *Malat1* and *Neat1* nascent RNAs are each processed by RNases P and Z to produce nuclear-retained ncRNAs and small cytoplasmic RNAs (*mascRNA* from *Malat1*, *menRNA* from *Neat1*) that exhibit a tRNA-like structure (Sunwoo et al., 2009; Wilusz et al., 2008) (Figure 1D). RNA fluorescence in situ hybridization (FISH) demonstrated that *Neat1* RNA localizes to nuclear regions in close proximity to *Malat1* RNA in mouse embryo fibroblasts (MEFs) as well as interstitial cells of testis (Figures 1E and 1F), consistent with the previously reported localization of these RNAs in nuclear speckles (*Malat1*) and paraspeckles (*Neat1*) of cultured cells (Clemson et al., 2009; Hutchinson et al., 2007; Mao et al., 2011; Sasaki et al., 2009; Sunwoo et al., 2009). Northern blot analyses showed that both *Malat1* and *Neat1* are nuclear retained in MEFs (Figure 1G), consistent with previous findings (Hutchinson et al., 2007), and that both *mascRNA* and *menRNA* are detected in mouse liver (Figure 1H) and kidney (data not shown). In contrast to a previous finding indicating that *menRNA* is unstable in cultured cells due to a noncanonical CCACCA addition at its 3′ end (Wilusz et al., 2011), our data suggest that *menRNA* generated in liver and kidney is a stable small RNA exhibiting the classical CCA addition (Figure S1). However, in wild-type mouse brain, while we

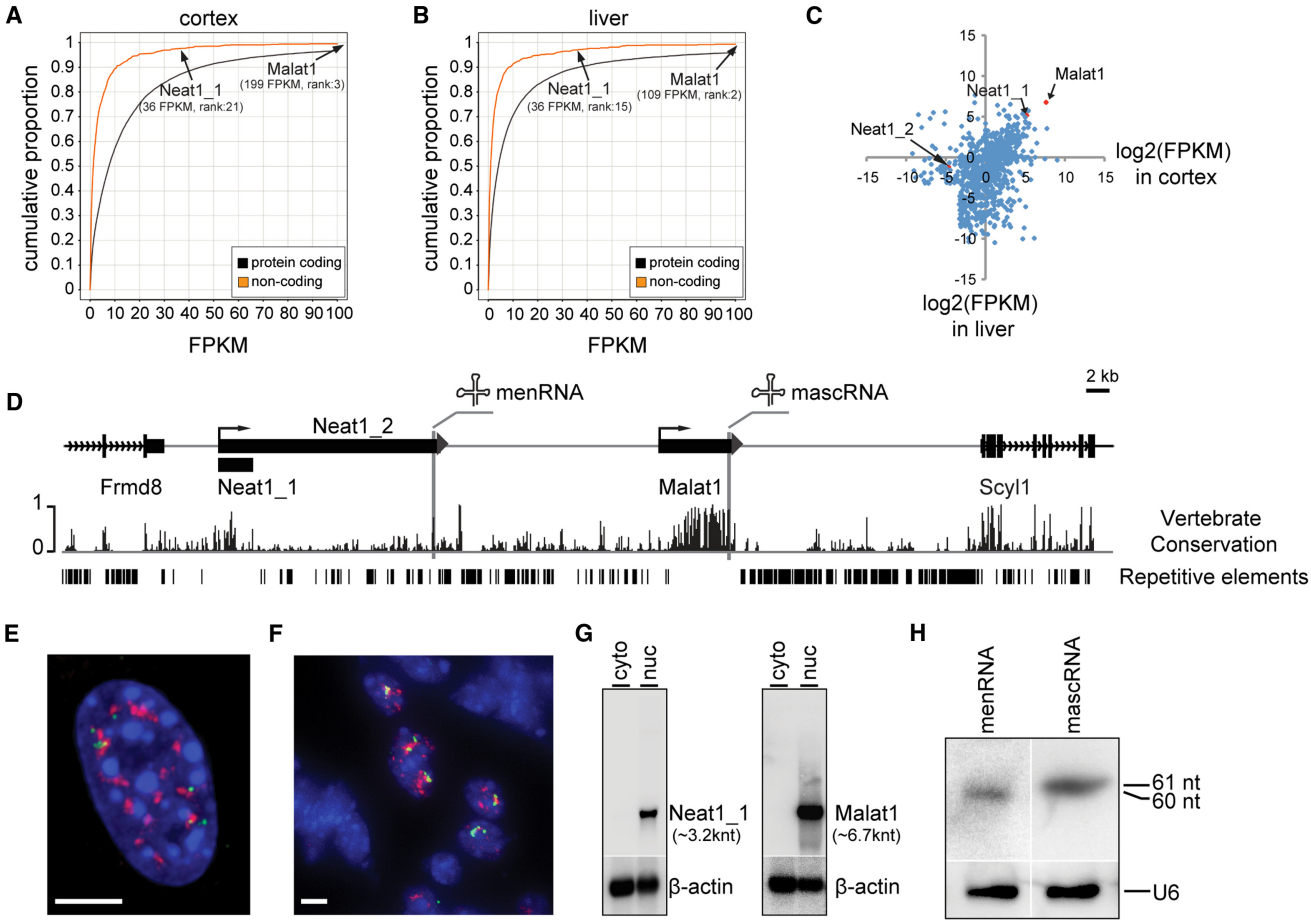

Figure 1. *Malat1* Encodes a Highly Abundant lncRNA in Vertebrates

(A and B) RNA-seq transcriptome analyses of mouse brain cortex and liver. Note that *Malat1* and *Neat1_1* are among the most abundant lncRNAs and that expression of *Malat1* in both cortex and liver is higher than that of most protein-coding genes.

(C) Tissue-specific expression of lncRNA genes. x and y axes indicate log2(FPKM) values of lncRNAs in cortex and liver, respectively.

(D) The reverse strand of the genomic locus of mouse chr19:5,760,586-5,860,585. *Malat1* is ~40 kb downstream of *Neat1*. *Frmd8* and *Scyl1* are adjacent protein-coding genes.

(E and F) RNA FISH shows that both *Malat1* (red) and *Neat1* (green) occupy distinct subnuclear domains in MEFs (E) and interstitial cells of testis (F). Blue, DAPI staining. Scale bars represent 5 μm.

(G) Northern blot analysis shows that *Neat1_1* and *Malat1* are enriched in the nuclear fraction and that β-actin is distributed in both cytosolic and nuclear fractions.

(H) Small RNA northern blot analysis shows that *menRNA* and *mascRNA* are detected in mouse liver. U6 is the loading control. Note that the blot in (H) is the same as that used in lanes 3 and 4 in Figure 3E to avoid cross-hybridization of the *menRNA* probe to *mascRNA*.

saw relatively high level of *mascRNA*, *menRNA* is not detectable (data not shown). This is most likely due to the lower expression of the long isoform of *Neat1* (*Neat1_2*) in brain, as observed by northern blot (data not shown) and RNA-seq analyses (*Neat1_2*: 0.44 FPKM in liver, 0.04 FPKM in cortex; Figure 1C). Collectively, our results demonstrate that *Malat1* lncRNA is expressed at a very high level, processed at its 3′ end to generate *mascRNA*, and localized in distinct subnuclear domains in mouse tissues as well as cultured cells.

Antisense Knockdown of *Malat1* ncRNA in Adult Mice Does Not Alter Organ Organization

The high abundance, strong evolutionary conservation, specific subcellular localization, and developmental regulation of *Malat1* suggest significant in vivo biological functions. However, such function could be derived from either the *Malat1* RNA transcript itself or the act of transcriptional activity of the *Malat1* gene. To distinguish between these two possibilities, we first examined the functional consequence of in vivo depletion of *Malat1* lncRNA. *Malat1* ASOs were administered into adult mice subcutaneously and the knockdown efficiency was examined by quantitative RT-PCR (qRT-PCR) and RNA in situ hybridization (ISH) (Figures 2A–2H). As compared with saline-treated animals, significant *Malat1* knockdown was observed in both liver (97%–98% knockdown; Figure 2G) and small intestine (86%–95% knockdown; Figure 2H) from animals treated with *Malat1* ASO1 or ASO2. Knockdown of *Malat1* with either of these ASOs does not alter the overall expression level of

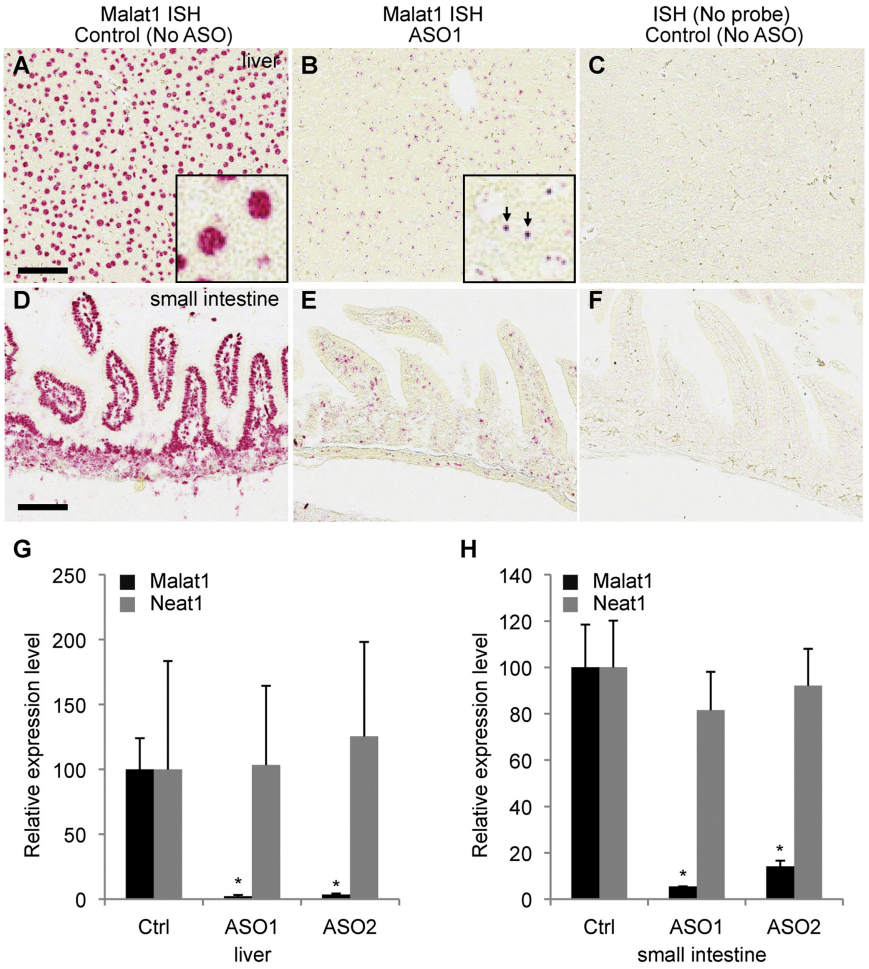

Figure 2. Antisense Knockdown of *Malat1* lncRNA in Adult Mice Does Not Alter Organ Organization

(A and B) ISH analysis of *Malat1* on saline-treated or *Malat1* ASO1-treated livers. *Malat1* is highly expressed in most liver cells (A), with its signal enriched in nuclei (inset of A). ASO1 efficiently knocks down *Malat1* expression in most liver cells (B), and the remaining signals form a few distinctive dots in nuclei (arrows, inset of B), which are most likely the nascent transcripts at the transcription sites of the *Malat1* gene locus.

(C) As a negative control, probe-free ISH on the saline-treated liver shows no hybridization signal.

(D and E) ISH analysis of *Malat1* on saline-treated or *Malat1* ASO1-treated small intestine. *Malat1* is highly expressed in most small intestine cells (D), with its signal enriched in nuclei. ASO1 efficiently knocks down *Malat1* expression in most cell types (E).

(F) As a negative control, probe-free ISH on the saline-treated small intestine shows no hybridization signal. Scale bars represent 100 μm.

(G and H) qRT-PCR analyses show that *Malat1* ncRNA is significantly knocked down in ASO-treated liver (G) and small intestine (H), while *Neat1* ncRNA exhibits no significant change upon *Malat1* depletion in both liver (G) and small intestine (H). ISH, in situ hybridization; ASO, antisense oligonucleotide; Ctrl, control. Error bars represent SD. *$p < 0.05$, Student's unpaired t test.

Neat1 in liver or small intestine (Figures 2G and 2H). ASO1 was slightly more effective than ASO2 in both liver and small intestine. In liver, *Malat1* depletion in hepatocytes was more dramatic than in bile duct epithelial cells (data not shown). In small intestine, *Malat1* knockdown in villi epithelial cells was more effective than in crypts and lamina propria (Figures 2D–2F). No detectable *Malat1* signal was observed in saline-treated tissues incubated without *Malat1* probes (Figures 2C and 2F). Although significant knockdown was achieved, no noticeable abnormality was seen in serum chemistry and tissue morphology between *Malat1* ASO and control, PBS-treated mice.

Generation and Characterization of a *Malat1*$^{-/-}$ Mouse Model

As in vivo knockdown studies did not reveal a function for *Malat1* lncRNA in adult mice, we developed a knockout mouse to delineate its potential role during early development and to assess whether the direct function of the *Malat1* gene is the act of its transcription. Toward this end, we generated *Malat1* mutant mice using homologous recombination in ESCs (Figure 3A). We found the recombination rate at the *Malat1* locus to be ~36% (24 recombination positives from 67 clones), higher than other loci in the genome. This is consistent with previous reports of the high susceptibility for translocation and DNA damage, and an exceptionally high transcriptional activity at the *Malat1* locus (Davis et al., 2003; Ferris et al., 2010; Kato et al., 2012; Rajaram et al., 2007).

The mutant mice, lacking a ~3 kb genomic region containing the 5′ end of the *Malat1* gene and its promoter, were genotyped by Southern blotting and tail DNA PCR analyses (Figures 3B and 3C). Northern blotting analysis using a ~2 kb partial cDNA probe showed that the *Malat1* transcript is completely depleted in *Malat1*$^{-/-}$ tissues (Figure 3D). In addition, small RNA northern blotting analysis using an oligonucleotide probe demonstrated that *mascRNA* is absent in *Malat1*$^{-/-}$ kidney and liver, but is detectable in *Malat1*$^{-/-}$ brain at a significantly lower level as compared to that in wild-type brain (Figure 3E). The minimal amount of *mascRNA* in mutant brain may be the result of a transcript derived from a brain-specific promoter upstream of the 3′ tRNA-like structure. However, we did not see any other RNA bands of a different size recognized by a *Malat1* partial cDNA probe in both wild-type and mutant brains (Figure 3D).

Since knockdown of *Malat1* in human HeLa cells was previously shown to result in alterations in alternative pre-mRNA splicing and cell death (Tripathi et al., 2010), we expected that homozygous deletion of *Malat1* would result in aberrations in pre- and/or postnatal development or tissue maturation. However, *Malat1*$^{-/-}$ mice are grossly normal and fertile. The

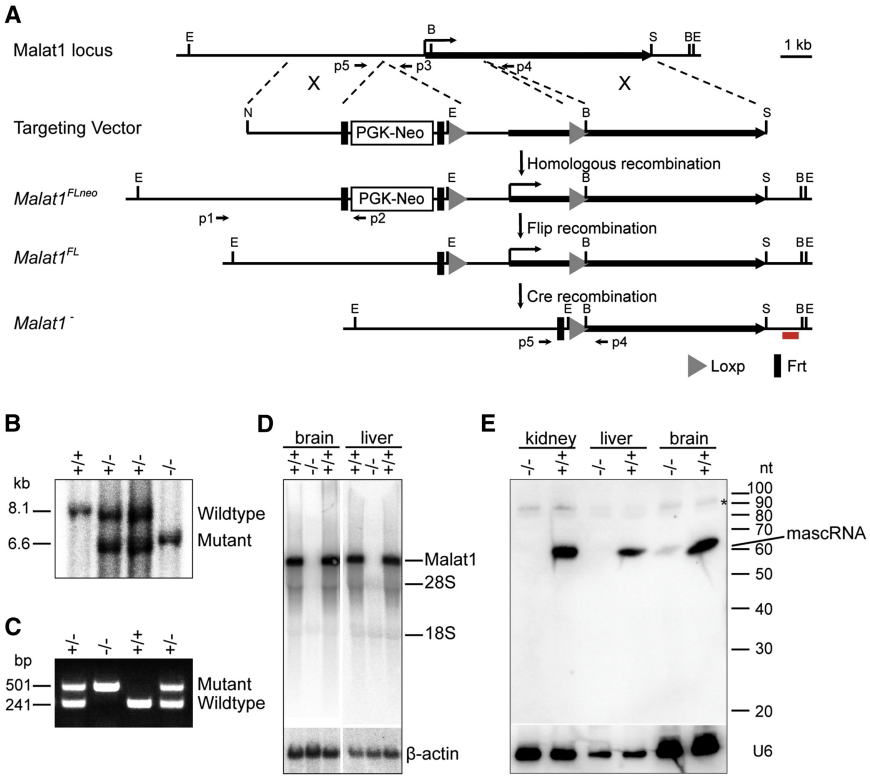

Figure 3. Generation and Characterization of a *Malat1* Knockout Mouse

(A) The strategy for *Malat1* targeting using homologous recombination. E, *EcoR*I; S, *Sal*I; N, *Not*I; B, *Bgl*II; X, homologous recombination; p1, p2, p3, p4, p5, PCR primers; red line, 3′ external probe for Southern blot analysis.

(B and C) Southern blot (B) and PCR (C) analyses show detection of wild-type and *Malat1* mutant alleles.

(D) Northern blot analyses show that *Malat1* lncRNA is depleted in homozygous mutant brain and liver. 28S and 18S indicate the positions of their size.

(E) Small RNA northern blot analyses using oligo probe show that *mascRNA* is depleted in *Malat1* mutant liver and kidney and that a small amount of *mascRNA* is detected in the mutant brain. *, nonspecific bands. β-actin and U6 are the loading controls.

offspring of heterozygous breedings follow Mendelian segregation (Figure S2A), suggesting that deletion of *Malat1* does not affect mouse pre- and postnatal viability. Breedings between *Malat1* homozygotes and wild-type produce normal-sized litters (Figure S2A), indicating that *Malat1*$^{-/-}$ mice are fertile. A large number of tissues from wild-type and mutant mice were assessed for potential histopathological alterations upon *Malat1* deletion. No obvious gross phenotypes were observed in mutants (Figures S2B–S2G). Blood cell counts and chemistry did not show any significant defects in *Malat1* mutant mice (data not shown). We also performed immunohistochemical labeling of Ki67 and Cleaved Caspase3 and did not see any significant difference in terms of the number of proliferating or apoptotic cells between wild-type and mutant tissue sections (data not shown). This is in stark contrast to cell death and growth arrest induced by *Malat1* knockdown using ASOs or RNAi in human and mouse cell lines (Tripathi et al., 2010; Yang et al., 2011). Together, these data suggest that neither *Malat1* nor its transcription is essential for mouse development, viability, and fertility under normal physiological and environmental conditions. However, it remains to be determined whether *Malat1* and/or its transcriptional activity are required under specific stress conditions or whether functional redundancy exists in the mouse.

Malat1 lncRNA Is Not Necessary for the Establishment or Maintenance of Nuclear Speckles

Malat1 lncRNA localizes to nuclear speckles and interacts with nuclear-speckle-associated proteins such as SRSF1 (Hutchinson et al., 2007; Tripathi et al., 2010), suggesting a potential function for *Malat1* in nuclear speckle assembly and/or maintenance. To investigate the effects of loss of *Malat1* lncRNA on nuclear speckles, we isolated MEFs. No proliferation or apoptotic defects were seen in mutant MEFs as compared to wild-type (data not shown). RNA FISH and qRT-PCR analyses indicated that *Malat1* lncRNA is completely depleted from the mutant MEFs while its neighboring lncRNA *Neat1* is slightly upregulated and forms two paraspeckle clusters, presumably around its transcription sites (Figures 4A–4C).

To examine whether loss of *Malat1* lncRNA affects nuclear speckle or paraspeckle morphology, we performed immunofluorescence (IF) labeling for these nuclear domains, using antibodies against SRSF2 and PSP1α in MEFs. We found that *Malat1* deletion has no overall effect on the number, size, and distribution of either nuclear speckles (Figures 4D and 4E) or paraspeckles (Figure S3).

Loss of *Malat1* Does Not Alter the Level and/or Phosphorylation Status of SR Proteins

Nuclear speckles are characterized by the enrichment of pre-mRNA splicing factors, including those of the SR family and small nuclear ribonucleoprotein complexes (reviewed in Lamond and Spector, 2003). It has been previously reported that *Malat1* knockdown in HeLa cells alters the level and phosphorylation status of two SR proteins, resulting in changes in the alternative splicing pattern of certain pre-mRNAs, and significant G2/M arrest and cell death (Tripathi et al. 2010). Since *Malat1* mutant mice are fertile and do not exhibit any obvious cellular or tissue defects, we examined the phosphorylation status of SR family members in wild-type versus mutant mice. Initially, the status of SR protein phosphorylation in MEFs was evaluated by immunoblot and probing against members of the SR family, including SRSF1, with the use of a phospho-epitope specific antibody (3C5) that recognizes the conserved serine arginine residues of

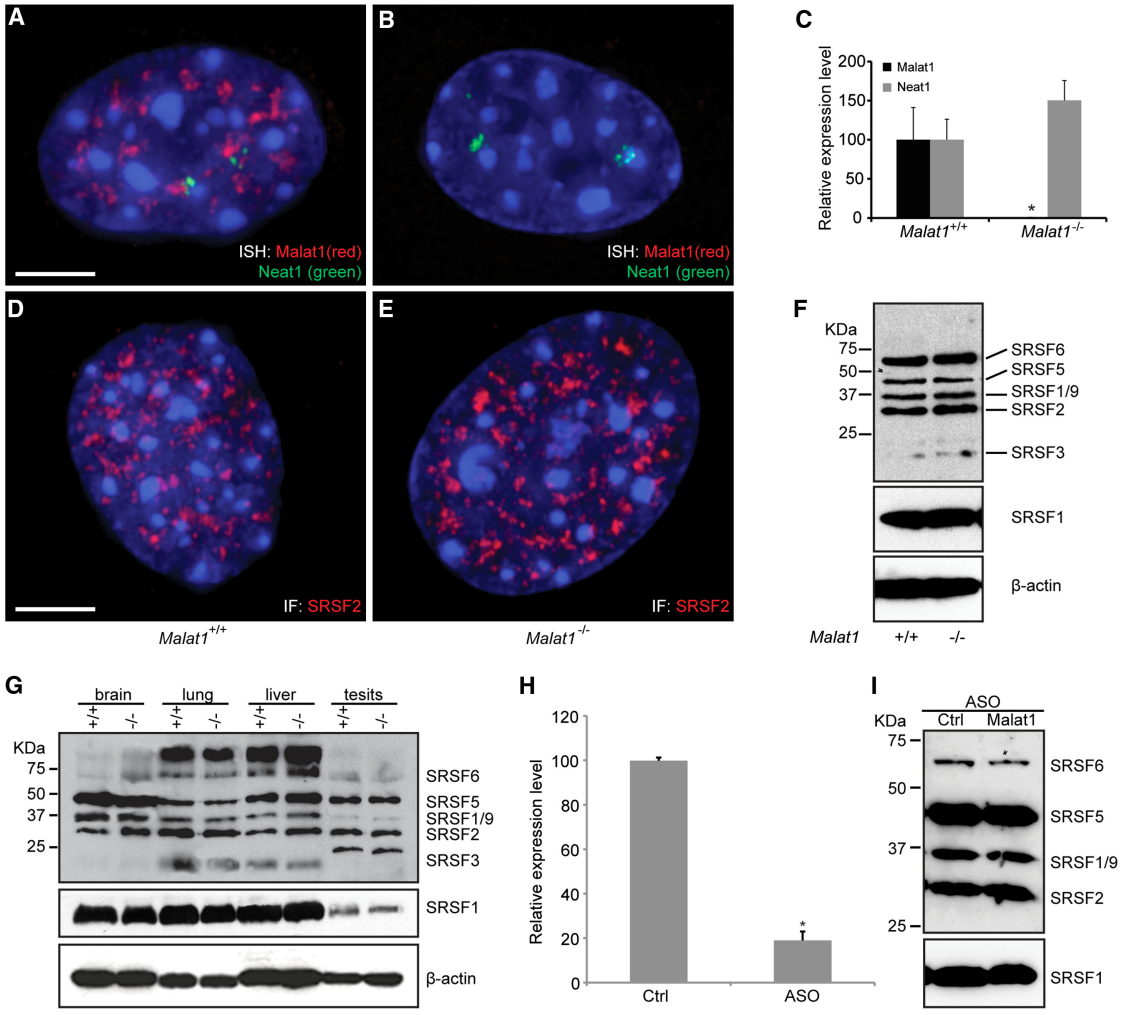

Figure 4. Depletion of *Malat1* lncRNA Does Not Alter *Neat1* Localization or Nuclear Speckle Morphology or the Phosphorylation Status of SR Proteins

(A and B) RNA FISH shows the subnuclear distribution of *Malat1* (red) and *Neat1* (green) in wild-type (A) and *Malat1*$^{-/-}$ (B) MEFs. Note that *Neat1* ncRNAs form two nuclear clusters adjacent to *Malat1* ncRNAs. Blue, DAPI staining.

(C) qRT-PCR analysis shows that *Malat1* ncRNA is depleted in *Malat1*$^{-/-}$ MEFs, while *Neat1* ncRNA exhibits no significant change in the mutants as compared to wild-type. Error bars represent SD. *$p < 0.05$, Student's unpaired t test.

(D and E) Immunofluorescence labeling of SRSF2(SC35) for nuclear speckles shows no significant changes of nuclear speckle morphology, distribution, and number in the mutant (E) as compared to wild-type (D) MEFs. Blue, DAPI staining.

(F) Western blot analyses of phospho SR proteins labeled by 3C5 antibody and total SRSF1 labeled by anti-SRSF1 show no change of SR protein level or phosphorylation status in the mutant as compared to wild-type MEFs. β-actin is the loading control. Scale bars represent 5 μm.

(G) Western blot analyses of phospho SR proteins show no changes of SR protein phosphorylation status or total SRSF1 level in brain, lung, liver, and testis from the mutant as compared to wild-type. β-actin is the loading control.

(H) qRT-PCR analysis shows that free-uptake ASO against *MALAT1* knocks down *MALAT1* lncRNA by ~80% compared to the control ASO (Ctrl) in MCF7 cells. Error bars represent SD. *$p < 0.05$, Student's unpaired t test.

(I) Western blot analyses of phospho SR proteins show no changes of SR protein phosphorylation status or protein level in MCF7 cells treated with the *MALAT1* ASO compared to the control ASO (Ctrl).

SR family members of splicing factors (Turner and Franchi, 1987). We did not observe any alteration in the level or phosphorylation status of SR proteins, including SRSF1, in *Malat1*$^{-/-}$ MEFs as compared to wild-type (Figure 4F).

Next, we examined the phosphorylation status of these SR proteins in adult tissues of wild-type and mutant mice, and we found that there is no change in the total pool of phosphorylated splicing factors and that the level of SRSF1 remained the same in each of the tissues (adult brain, lung, liver, and testis) of wild-type and *Malat1* mutant samples (Figure 4G). Immunofluorescence of SRSF2 in wild-type and mutant MEFs also did not show any change in nuclear speckle number or morphology (Figures 4D and 4E). The speckled pattern was also studied in adult mouse tissue sections by immunofluorescence using SRSF2 antibody,

and cells exhibited no change in the number or pattern of nuclear speckles in *Malat1*$^{-/-}$ tissues as compared to wild-type (data not shown). These observations clearly demonstrate that *Malat1* loss does not result in a change in the level or phosphorylation status of SR splicing factors or the association of SRSF2 with nuclear speckles in vivo.

This was very surprising, given the fact that in HeLa cells, knockdown of *Malat1* had a profound effect on splicing factor phosphorylation status (Tripathi et al., 2010). As *Malat1* is among the most conserved lncRNAs in mammals, it is highly unlikely that it will have a different function between mouse and human. To address this discrepancy, we repeated the *Malat1* knockdown experiment in human HeLa cells by using lipofectamine 2000-mediated transfection of ASOs. While knockdown of *Malat1* at 48 hr and 72 hr after transfection resulted in dephosphorylation of SRSF1 (Figure S4) accompanied by significant cell death, SRSF1 phosphorylation changes and cell death were also observed at some level in control ASO-transfected cells 72 hr after treatment. However, similar knockdown experiments using Fugene, a less toxic lipid reagent, resulted in no significant cell death after 48 hr and minimal cell death after 72 hr in both control ASO and *MALAT1* ASO treated human MCF7 cells (data not shown). To further confirm that knockdown of *MALAT1* in cultured cells does not cause cell death and alter SR phosphorylation status, we used ASOs with a MOE gapmer structure, which can be taken up effectively by some cultured cell lines without transfection reagents. The *MALAT1* knockdown using ASOs at 75 nM concentration in MCF7 cells reached a level of 80%–90% RNA reduction after 48 hr (Figure 4H), which is comparable to that of ASO knockdown using lipid transfection reagents. The *MALAT1* knockdown by free uptake ASOs did not alter the phosphorylation status of SR proteins and the SRSF1 level at the 48 hr time point in MCF7 cells (Figure 4I) and did not result in cell death at the 72 hr time point (data not shown). We also see no effects of *Malat1* knockdown on SR phosphorylation in human SW480 (Figure S4) and MCF10A cells or in mouse mammary tumor 4T1, 4T07, 67NR, and 168FARN cells (data not shown). Taken together, *MALAT1* loss in and of itself does not result in changes in the level of SRSF1 or the phosphorylation status of SR proteins, or in cell death in many human and mouse cell lines as well as in mouse tissues.

Malat1 lncRNA Does Not Regulate Global Pre-mRNA Splicing

While depletion of *Malat1* RNA in mouse tissues does not alter nuclear speckle morphology or cause any significant changes in SR protein level and phosphorylation, we were interested in examining the effect of loss of *Malat1* on global gene expression and alternative pre-mRNA splicing. To probe molecular changes in *Malat1* mutant tissues, we performed RNA-seq profiling and obtained ~70 million paired-end reads for each sample (liver: 3 wild-types and 3 mutants; brain cortex: 3 wild-types and 3 mutants; data from wild-type were used for the lncRNA abundance quantification in Figure 1). We examined all (~13,000) cassette exons annotated in the mouse genome, which represent the most predominant pattern of alternative splicing, and did not see global changes in the average inclusion level between wild-type and *Malat1* mutant livers (Figure S5A and Figure 5A) or cortices (Figure S5B and Figure 5B). Only ten exons in liver and five exons in brain cortex show statistically significant changes (false discovery rate [FDR] < 0.05 and $|\Delta I| > 0.1$; see Experimental Procedures; Figures 5A and 5B), of moderate magnitude and sometimes with substantial variation between biological replicates. Therefore, *Malat1* does not appear to regulate global pre-mRNA splicing in adult mouse liver and brain cortex.

Inactivation of *Malat1* Transcription Alters Local but Not Global Gene Expression

It has been recently reported that *Malat1* interacts with unmethylated Pc2 to promote E2F1 SUMOylation, resulting in relocation of its downstream growth-control genes to nuclear speckles for expression, and that knockdown of *Malat1* inhibits cell growth with a failure of these genes to reposition in the nucleus (Yang et al., 2011). *Malat1* knockdown has also been shown to alter several synaptogenesis-associated genes in cultured Neuro2A neuroblastoma cells (Bernard et al., 2010). To address whether *Malat1* regulates global gene expression, we compared expression levels of ~1,700 lncRNAs and ~19,000 protein-coding genes in wild-type and mutant livers and brain cortices (see Experimental Procedures). Interestingly, *Malat1* lncRNA is absent in mutant liver (wild-type, 109 FPKM; mutant, 0.1 FPKM) (Table S2) but still detectable at a very low level in mutant brain cortex (wild-type, 199 FPKM; mutant, 2 FPKM) (Table S3). RNA-seq reads of *Malat1* in mutant brain cortex were mapped to a ~3 kb region upstream of *mascRNA* (data not shown), consistent with the presence of a low level of *mascRNA* in mutant brain cortex (Figure 3E). It remains to be determined whether this 3 knt transcript is expressed by an alternative promoter to compensate for the loss of full-length *Malat1* in mutant brain.

In both liver and cortex, no significant global changes in steady-state mRNA level were detected (Figures 5C and 5D). After multiple testing correction, only one gene (*Saa3*, serum amyloid A 3) in liver and 12 genes in cortex showed statistically significant changes between wild-type and *Malat1* mutants (Tables S2 and S3). However, we observed a bigger sex difference of gene expression in liver than in cortex (data not shown), which might have masked some changes. For example, *Neat1* shows higher expression in males and consistent ~1.5- to 2-fold increases in *Malat1* mutant livers in both sexes (Figures S6A and S6B and Table S4A). When we compared gene expression in livers only from males, 22 genes, including *Saa3* and *Upp2* (uridine phosphorylase 2), have statistically significant changes between wild-type and *Malat1* mutant liver samples (Table S2).

Interestingly, among the 12 genes with significant expression changes in brain cortex, five are adjacent to *Malat1*, including *Neat1*, *Frmd8*, *Tigd3*, *Ehbp1l1*, and *Ltbp3* (Figures 5E–5G; Table S4B). All of these genes are upregulated 1.5- to 2.3-fold upon inactivation of the *Malat1* gene (Table S3). Upon further examination of other genes adjacent to *Malat1* (~240 kb region centered around *Malat1*), we found seven additional genes, *Map3k11*, *Kcnk7*, *Fam89b*, *Scyl1*, *Slc25a45*, *Dpf2* and *Cdc42ep2* whose upregulation reaches statistical significance without genome-wide multiple-testing correction (1.15- to 1.3-fold; Figure 5H;

Cell PRESS
Open ACCESS

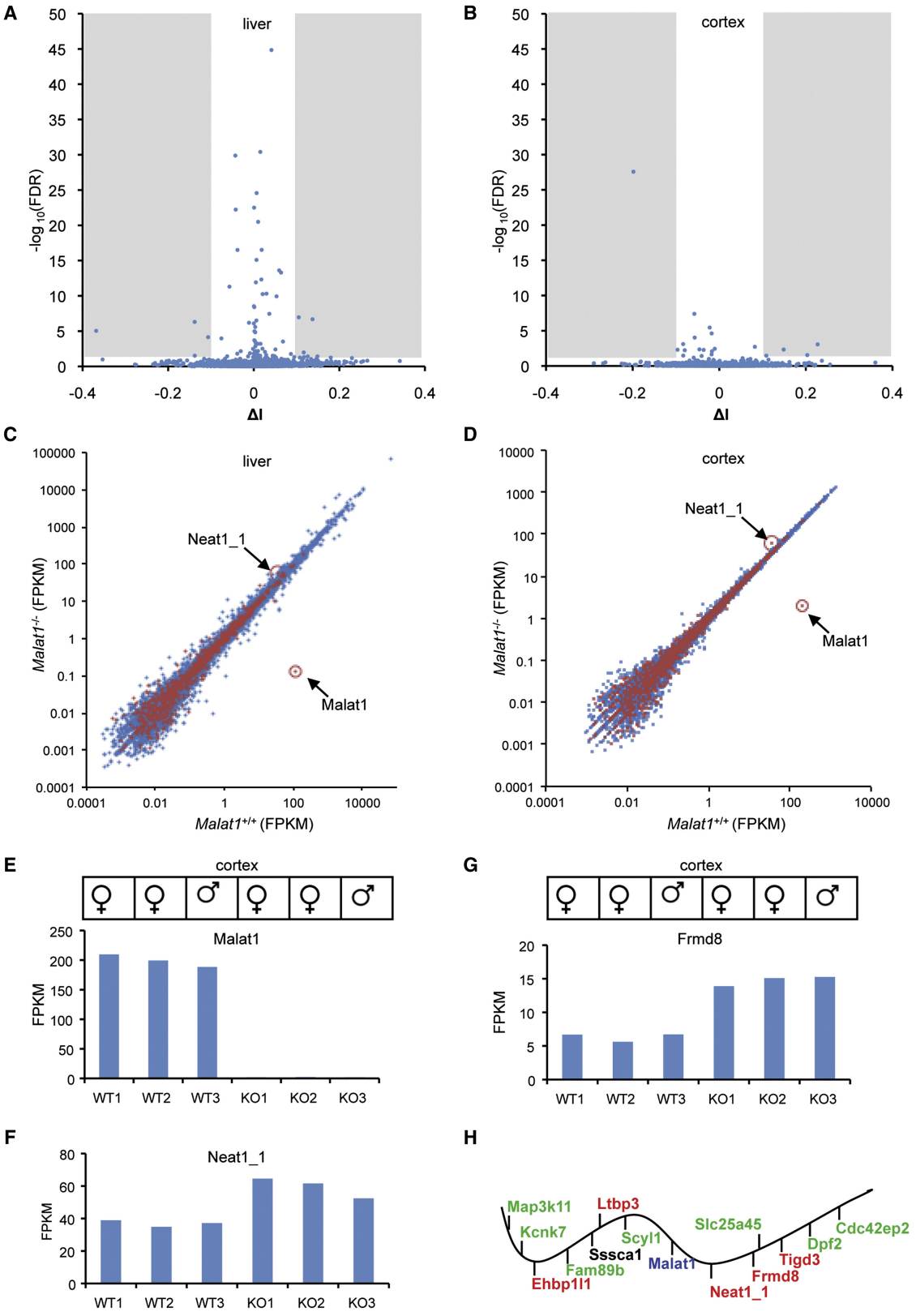

Table S4B). Collectively, our data demonstrate that inactivation of the *Malat1* gene upregulates gene expression in *cis* but does not alter global gene expression patterns in mouse liver and cortex.

DISCUSSION

Genome-wide approaches have been successfully applied to identify thousands of lncRNAs, some of which are transcribed spatiotemporally. A complete understanding of their in vivo function(s) requires molecular and cell biological characterization as well as the development of genetic models to assess their role(s) at the more complex organismal level. Here, we have developed a loss-of-function genetic model for *Malat1*, one of the most well conserved and highly expressed lncRNAs. While *Malat1* does not have a direct role in mouse pre- and postnatal development, inactivation of its transcription results in an upregulation of a small number of adjacent genes.

Malat1 nascent transcripts are processed by RNases P and Z to produce a 6.7-knt-long nuclear-retained ncRNA with a genomically encoded short polyA-like moiety at its 3′ end and a tRNA-like small RNA, *mascRNA* (Wilusz et al., 2008), that is transported to the cytoplasm. Although *Malat1* is highly abundant in polyA(+) samples, given its lack of a traditional poly(A) tail, it is very likely that our RNA-seq analysis of such samples underestimates the abundance of *Malat1*. Consistent with this, it has been reported that ~0.4%–2.0% total sequencing reads from the transcriptome profiling for ribo (−) RNA species in a number of mouse tissues are mapped to the *Malat1* gene (Castle et al., 2010), indicating the high abundance and wide expression pattern of this lncRNA.

The *Malat1* gene is located on mouse chr.19qA (human chr.11q13.1). Interestingly, ~40 kb upstream of *Malat1* in the mouse genome, another lncRNA gene, *Neat1,* produces two isoforms with different 3′ ends. The short *Neat1* transcript (*Neat1_1*) is 3.2 knt, while the nascent long *Neat1* transcript (*Neat1_2*) is also processed by the tRNA processing machinery to produce a nuclear retained ~20-knt-long *Neat1_2* transcript and *menRNA*, a small tRNA-like RNA (Sunwoo et al., 2009). In mammalian genomes, the primary sequences of both *Malat1* and *Neat1_1* are highly conserved and are nearly devoid of annotated repeat-derived sequences, implying biological functions of these RNAs. *Neat1* is not computationally detected outside of mammals; however, the *Malat1* gene is syntenically conserved in most sequenced gnathostome genomes (Stadler, 2010). Except for the conserved 3′ end processing module, the rest of *Malat1* lncRNA is surprisingly divergent, without homologous fragments detected between fishes and mammals. Interestingly, similar to that observed in human and mouse, the transcriptional activity of the *Malat1* gene in lizard, *Xenopus*, and zebrafish is exceptionally high (B.Z. and D.L.S., unpublished data; Ulitsky et al., 2011), suggesting that maintaining the high transcriptional activity of the *Malat1* locus during evolution may be important. The strong constraint on the 3′ end processing module during the evolution of gnathostomes implies that the processing mechanism and/or its products may carry a biological role. However, the functional carrier for the *Malat1* locus during evolution is not necessarily limited to only one component. Instead, it is very likely to be combinations of the lncRNA transcript, the transcription of the *Malat1* gene, and/or the small *mascRNA.*

The chromatin structure at the *Malat1-Neat1* genomic locus exhibits several interesting features. (1) Transcription of these two lncRNA genes is very active (Castle et al., 2010), and in some cell types, RNA Pol II binding at their promoters is extremely high as compared to the entire genome (Martianov et al., 2010). (2) The human 11q13 region, where human *MALAT1* is located, is a ''RIDGE'' chromosome domain of very high gene density and gene expression that supports strong transcription activity of inserted transgenes (Gierman et al., 2007) and has a very decompact higher-order chromatin structure (Gilbert et al., 2004). (3) The homologous recombination frequency is exceptionally high for both *Malat1* (this study) and *Neat1* (B.Z. and D.L.S., unpublished data). (4) *Malat1* is frequently translocated in renal carcinoma and embryonic sarcoma (Davis et al., 2003; Rajaram et al., 2007). (5) *Malat1* is the most favored hotspot for HIV integration mediated by the ING2–IBD fusion (Ferris et al., 2010) and is among the top targets of activation-induced cytidine deaminase (AID) with accumulated mutations as frequent as the Ig locus after AID activation in B cells (Kato et al., 2012). Taken together, the high susceptibility for recombination, translocation, and DNA breaks is most likely associated with a distinct chromatin structure and/or histone modifications of the locus, which is responsible for its high transcriptional activity. Given these characteristics, this genomic locus could be utilized to efficiently knock in any transgene of interest to achieve stable and high expression in most tissues and cell types.

The specific subcellular localization of *Malat1* has led some to suggest that this RNA could function along with speckle-associated protein factors (i.e., SRSF1 and SRSF2) and other nuclear proteins to regulate cell- and tissue-specific gene expression and/or pre-mRNA splicing. In this regard, two recent studies

Figure 5. *Malat1* RNA Does Not Regulate Global Pre-mRNA Splicing, but Its Transcription Inactivation Alters Gene Expression in *cis*

(A and B) The volcano plot shows proportional change of inclusion level (x axis, ΔI) of each exon and their statistical significance [y axis, −log10(FDR)] upon *Malat1* depletion. Shaded regions represent statistically significant changes.

(C and D) The scatterplot shows the average expression of protein-coding (blue) and lncRNA (red) genes in wild-type and *Malat1* mutant livers and brain cortices. *Malat1* and *Neat1_1* are highlighted.

(E) *Malat1* is significantly depleted in *Malat1* mutant brain cortexes.

(F and G) *Neat1_1* and *Frmd8* show consistent overexpression in mutant cortexes. WT, wild-type (*Malat1*$^{+/+}$); KO, knockout (*Malat1*$^{-/-}$).

(H) The ~240 kb genomic locus of *Malat1*, with adjacent genes distributed in order but not at the exact scale. Upregulated genes with statistical significance after multiple testing correction (red) and with statistical significance without multiple-testing correction (green). *Sssca1* expression is not significantly altered. Vertical bars under the wavy line represent transcription from the negative strand of the chromosome; vertical bars above the line represent transcription from the positive strand.

have revealed different phenotypes upon *Malat1* knockdown in HeLa cells. Tripathi et al. (2010) demonstrated that knockdown of *Malat1* resulted in a G2/M phase arrest and significant levels of cell death in both human HeLa cells and mouse EpH4 cells (Tripathi et al., 2010). Contrary to this finding, Yang et al. (2011) showed that *Malat1* depletion resulted in a G1/S phase arrest (Yang et al., 2011). However, we have found that *Malat1* knockout mice are viable and fertile, with no obvious gross abnormalities, and their cells do not exhibit increased cell death or defects in cell-cycle progression. This discrepancy of *Malat1* function between in vitro and in vivo analyses could be due to redundant compensatory mechanisms during development; however, the transient knockdown of *Malat1* in adult mouse tissues and cultured cells by free uptake of ASOs in the absence of any transfection reagent did not induce either cell death or cell-cycle arrest.

The different cellular phenotypes observed in *Malat1*-depleted HeLa cells, G2/M arrest/increased cell death versus G1/S arrest, were explained by distinct molecular mechanisms of *Malat1* in splicing versus gene expression, respectively (Tripathi et al., 2010; Yang et al., 2011). Tripathi et al. (2010) demonstrated that *Malat1* regulates pre-mRNA splicing through modulating the pre-mRNA splicing factor level and the phosphorylation status of one or more SR family splicing factors (Tripathi et al., 2010). In contrast, Yang et al. (2011) showed that *Malat1* interacts with unmethylated Pc2 to promote E2F1 target gene expression during cell-cycle progression (Yang et al., 2011). However, our cellular, biochemical, and molecular analyses showed no significant changes in the level and/or phosphorylation status of SR proteins or global splicing patterns in *Malat1*-depleted human and mouse cells and tissues. We also did not see global changes of steady-state mRNA levels or E2F1 target gene misregulation upon *Malat1* depletion in mouse liver and cortex. Furthermore, neither cell death nor alterations in proliferation were observed when *Malat1* was knocked down using free-uptake ASOs. Taken together, our data on mouse tissues and mouse and human cells suggest that loss of *Malat1* does not alter global pre-mRNA splicing and/or gene expression.

Although we did not observe changes in either global gene expression or alternative pre-mRNA splicing in the *Malat1* knockout mutants, we did identify a small number of genes with statistically significant changes in expression in liver and brain cortex. For example, *Neat1* is upregulated by ~1.5- to 2-fold in both liver and cortex, suggesting a potential compensation between *Malat1* and *Neat1*. Interestingly, among the 12 genes with statistically significant changes in expression level upon inactivation of the *Malat1* gene in brain cortex, five of these genes reside adjacent to *Malat1* and are upregulated by ~1.5- to 2.3-fold. Furthermore, several additional genes in the proximity of *Malat1* also showed significant upregulation when statistical analysis was performed without the use of a multiple-testing correction against the entire genome. This *cis* effect on gene expression is similar to the effect observed upon loss of imprinting lncRNAs, such as *Air* (Sleutels et al., 2002). However, so far there is no evidence in support of the role of the *Malat1* locus in imprinting. Since we did not see *Neat1* expression changes upon depletion of *Malat1* RNA by ASO treatment in liver and small intestine, this *cis* effect is probably not mediated by *Malat1* RNA itself, implying a different mechanism than imprinting. The syntenic conservation and strong transcription of the *Malat1* locus from fish to human suggest that transcription of the *Malat1* gene may carry a function that is under selective constraints during evolution. This may also explain why the *Malat1* primary sequence is very divergent between fish and human except for the 3′ end tRNA-like processing module. Several mechanisms underlying ncRNA transcription-mediated *cis* gene regulation have been recently identified. It has been demonstrated that transcription of ncRNA genes can directly interfere with downstream or overlapping gene transcription by altering transcription factor binding at the yeast *SER3*, *FLO11,* and *IME4* loci (Bumgarner et al., 2012; Hongay et al., 2006; Martens et al., 2004) and the *Drosophila* Ubx locus (Petruk et al., 2006). This mechanism is called transcriptional interference, the direct negative influence of one transcriptional process on a second transcriptional process in *cis* (reviewed in Shearwin et al., 2005). Moreover, the act of ncRNA transcription can also induce histone modifications and thus indirectly alter the overlapping or neighboring gene transcription, as demonstrated at the budding yeast *PHO84* locus (Camblong et al., 2007), *GAL1-10* gene clusters (Houseley et al., 2008), and the *fbp1+* locus in *S. pombe* (Hirota et al., 2008). Given that a number of *Malat1* neighboring genes showed significant upregulation upon *Malat1* inactivation and that *Malat1* transcription does not overlap with any nearby protein-coding genes, the *cis* effect may be attributed to altered histone modification, which could have a broad impact on local chromatin organization. Alternatively, the strong *Malat1* promoter activity may sequester RNA pol II from its adjacent genes, thereby modulating their expression in wild-type cells. However, we cannot rule out the possibility that the deleted 3 kb region of the *Malat1* gene contains *cis* DNA elements that negatively regulate expression of genes adjacent to *Malat1*. In addition, given the distinct subnuclear localization and high abundance of the *Malat1* lncRNA and its conservation in mammals, it is highly likely that the *Malat1* transcripts will also exhibit a *trans* effect in mouse tissues under specific physiological conditions. Examining these possibilities merits future investigation.

Taken together, our in vivo and in vitro studies demonstrate that *Malat1* is not essential for mouse pre- and postnatal development and that its deletion does not affect global gene expression and pre-mRNA splicing under the conditions examined. Among a small number of genes with significant changes in expression in mouse liver and cortex, a significant number of these genes are *Malat1* neighboring genes. Despite being dispensable for development, the unique features of *Malat1*, syntenic conservation, high abundance, conserved 3′ end processing, specific nuclear localization, and developmental regulation, argue for a broader functional role for this lncRNA. A lack of phenotype upon the loss of *Malat1* lncRNA transcripts could be attributed to functional redundancy with other RNA transcripts (e.g., *Neat1* lncRNA) or to compensatory mechanisms during development, as occurs with respect to many protein-coding genes. Alternatively, some lncRNAs, including *Malat1*, could have a subtle role and regulate cellular processes via

a fine-tuning mechanism. Given the initial identification of *Malat1* as a gene whose upregulation was correlated with tumors that have the propensity to metastasize (Ji et al., 2003), it will be important to investigate the potential role of *Malat1* in cancer progression and upon other pathological stresses.

EXPERIMENTAL PROCEDURES

All animal protocols have been approved by the CSHL Animal Care and Use Committee.

In Vivo Knockdown of *Malat1*

Male Balb/c mice (n = 4) 7 weeks of age were subcutaneously dosed with saline, *Malat1* ASO1, or *Malat1* ASO2 (sequence information in Table S5) at 100 mg/kg/week for 4 weeks. At 24 hr after the last dose, the animals were sacrificed. The liver and small intestine were harvested and homogenized in RLT buffer (QIAGEN) containing 1% 2-mercaptoethanol. Total mRNA was prepared with the PureLink Total RNA Purification Kit (Invitrogen) according to the manufacturer's instruction. A second set of tissues were fixed in 10% buffered formalin for 72 hr and further paraffin embedded and sectioned at 4 μm for histology and RNA in situ hybridization analysis with the Affymetrix QuantiGene ViewRNA Assay.

Generation of *Malat1* Knockout Mice

Malat1-deficient mice were generated by homologous recombination, and genotypes were determined by Southern blot and PCR analyses (sequence information in Table S5; see details in Extended Experimental Procedures).

RNA-seq Expression and Splicing Analyses

Raw reads obtained from the Illumina pipeline were mapped back to the mouse reference genome (NCBI37/mm9) together with a comprehensive database of annotated exon junctions with the use of the program OLego (J.W. and C.Z., unpublished data, http://ngs-olego.sourceforge.net/). Only those reads that were mapped to unique loci with $\leq$ 4 mismatches (substitutions, insertions, or deletions) were used for further analysis. For junction reads, we required $\geq$ 8 nt matches on each side for novel junctions and $\geq$ 5 nt matches on each side for known junctions. Transcript structure of each cDNA fragment unobserved between the paired ends due to alternative splicing was then inferred with the use of a Bayes method, followed by analysis of alternative splicing in ~13,000 annotated cassette exons in the mouse genome (K. Charizanis and M.S. Swanson, unpublished data). In brief, fragments of the biological replicates were first pooled together, and cassette exons were then filtered by junction fragment coverage to reduce multiple testing (junction_in + junction_skip $\geq$ 20, junction_WT + junction_KO $\geq$ 20). A Fisher's exact test was performed to evaluate the statistical significance of splicing change using exon or exon-junction fragments, followed by Benjamini multiple-testing correction to estimate the FDR. In addition, proportional change of exon inclusion (ΔI) was calculated using inclusion or skipping junction fragments.

We analyzed the mRNA steady-state level of 18,974 protein-coding genes and 1,722 lncRNAs. For protein-coding genes, we defined a set of nonoverlapping "core" exons, which consists of a comprehensive collection of annotated exons in RefSeq and UCSC known genes, as well as in mRNA and EST sequences; exons showing an inclusion level < 0.5, as estimated from mRNA and EST data, were excluded. LncRNA genes were obtained from RefSeq on the basis of the annotated gene type "miscRNA." A vast majority of these ncRNAs in this collection are long and have multiple exons, but the collection also includes miRNAs and scaRNAs, which were excluded for this study. The remaining transcripts are from 1,722 unique loci, and all exons were used to estimate gene expression level. To estimate FPKM values, the number of fragments overlapping with exons in each gene was counted, normalized by the total length of core exons and the total number of exonic reads in all genes. Statistical significance of differential expression was assessed by the edgeR program (Robinson et al., 2010) using fragment counts in each sample.

SUPPLEMENTAL INFORMATION

Supplemental Information includes Extended Experimental Procedures, six figures, and five tables and can be found with this article online at http://dx.doi.org/10.1016/j.celrep.2012.06.003.

LICENSING INFORMATION

ACKNOWLEDGMENTS

We thank Carmen Berasain, Jan Bergmann, Megan Bodnar, Melanie Eckersley-Maslin, Stephen Hearn, Michael Hübner, Ileng Kumaran, Jingjing Li, Cinthya Zepeda-Mendoza, and Rui Zhao of the Spector laboratory and C. Frank Bennett at Isis Pharmaceuticals for helpful discussions and comments. We thank Sang Yong Kim, Alexey Revenko, Ying Lin, and Scilla Wu for technical assistance. We are grateful to Angus Lamond for PSP1α antibody and Adrian Krainer for SRSF1 antibody (AK96). This work was supported by grants from NCI 5P01CA013106-40, NCI 2P30CA45508-24, and NIGMS 42694 (to D.L.S.) and K99GM95713 (to C.Z.). B.Z. is supported by a Department of Defense Prostate Cancer Research Program postdoctoral fellowship (W81XWH-10-1-0190). Y.S.M. is supported by a National Cancer Center postdoctoral fellowship. D.L.S. is a consultant to Isis Pharmaceuticals.

Received: April 24, 2012
Revised: May 29, 2012
Accepted: June 7, 2012
Published online: June 28, 2012

REFERENCES

Bernard, D., Prasanth, K.V., Tripathi, V., Colasse, S., Nakamura, T., Xuan, Z., Zhang, M.Q., Sedel, F., Jourdren, L., Coulpier, F., et al. (2010). A long nuclear-retained non-coding RNA regulates synaptogenesis by modulating gene expression. EMBO J. *29*, 3082–3093.

Bumgarner, S.L., Neuert, G., Voight, B.F., Symbor-Nagrabska, A., Grisafi, P., van Oudenaarden, A., and Fink, G.R. (2012). Single-cell analysis reveals that noncoding RNAs contribute to clonal heterogeneity by modulating transcription factor recruitment. Mol. Cell *45*, 470–482.

Camblong, J., Iglesias, N., Fickentscher, C., Dieppois, G., and Stutz, F. (2007). Antisense RNA stabilization induces transcriptional gene silencing via histone deacetylation in S. cerevisiae. Cell *131*, 706–717.

Castle, J.C., Armour, C.D., Löwer, M., Haynor, D., Biery, M., Bouzek, H., Chen, R., Jackson, S., Johnson, J.M., Rohl, C.A., and Raymond, C.K. (2010). Digital genome-wide ncRNA expression, including SnoRNAs, across 11 human tissues using polyA-neutral amplification. PLoS ONE *5*, e11779.

Chen, L.L., and Carmichael, G.G. (2009). Altered nuclear retention of mRNAs containing inverted repeats in human embryonic stem cells: functional role of a nuclear noncoding RNA. Mol. Cell *35*, 467–478.

Chodroff, R.A., Goodstadt, L., Sirey, T.M., Oliver, P.L., Davies, K.E., Green, E.D., Molnár, Z., and Ponting, C.P. (2010). Long noncoding RNA genes: conservation of sequence and brain expression among diverse amniotes. Genome Biol. *11*, R72.

Clemson, C.M., Hutchinson, J.N., Sara, S.A., Ensminger, A.W., Fox, A.H., Chess, A., and Lawrence, J.B. (2009). An architectural role for a nuclear noncoding RNA: NEAT1 RNA is essential for the structure of paraspeckles. Mol. Cell *33*, 717–726.

Davis, I.J., Hsi, B.L., Arroyo, J.D., Vargas, S.O., Yeh, Y.A., Motyckova, G., Valencia, P., Perez-Atayde, A.R., Argani, P., Ladanyi, M., et al. (2003). Cloning of an Alpha-TFEB fusion in renal tumors harboring the t(6;11)(p21;q13) chromosome translocation. Proc. Natl. Acad. Sci. USA *100*, 6051–6056.

Ferris, A.L., Wu, X., Hughes, C.M., Stewart, C., Smith, S.J., Milne, T.A., Wang, G.G., Shun, M.C., Allis, C.D., Engelman, A., and Hughes, S.H. (2010). Lens epithelium-derived growth factor fusion proteins redirect HIV-1 DNA integration. Proc. Natl. Acad. Sci. USA *107*, 3135–3140.

Gierman, H.J., Indemans, M.H., Koster, J., Goetze, S., Seppen, J., Geerts, D., van Driel, R., and Versteeg, R. (2007). Domain-wide regulation of gene expression in the human genome. Genome Res. *17*, 1286–1295.

Gilbert, N., Boyle, S., Fiegler, H., Woodfine, K., Carter, N.P., and Bickmore, W.A. (2004). Chromatin architecture of the human genome: gene-rich domains are enriched in open chromatin fibers. Cell *118*, 555–566.

Guffanti, A., Iacono, M., Pelucchi, P., Kim, N., Soldà, G., Croft, L.J., Taft, R.J., Rizzi, E., Askarian-Amiri, M., Bonnal, R.J., et al. (2009). A transcriptional sketch of a primary human breast cancer by 454 deep sequencing. BMC Genomics *10*, 163.

Gupta, R.A., Shah, N., Wang, K.C., Kim, J., Horlings, H.M., Wong, D.J., Tsai, M.C., Hung, T., Argani, P., Rinn, J.L., et al. (2010). Long non-coding RNA HOTAIR reprograms chromatin state to promote cancer metastasis. Nature *464*, 1071–1076.

Guttman, M., Amit, I., Garber, M., French, C., Lin, M.F., Feldser, D., Huarte, M., Zuk, O., Carey, B.W., Cassady, J.P., et al. (2009). Chromatin signature reveals over a thousand highly conserved large non-coding RNAs in mammals. Nature *458*, 223–227.

Hirota, K., Miyoshi, T., Kugou, K., Hoffman, C.S., Shibata, T., and Ohta, K. (2008). Stepwise chromatin remodelling by a cascade of transcription initiation of non-coding RNAs. Nature *456*, 130–134.

Hongay, C.F., Grisafi, P.L., Galitski, T., and Fink, G.R. (2006). Antisense transcription controls cell fate in Saccharomyces cerevisiae. Cell *127*, 735–745.

Houseley, J., Rubbi, L., Grunstein, M., Tollervey, D., and Vogelauer, M. (2008). A ncRNA modulates histone modification and mRNA induction in the yeast GAL gene cluster. Mol. Cell *32*, 685–695.

Hutchinson, J.N., Ensminger, A.W., Clemson, C.M., Lynch, C.R., Lawrence, J.B., and Chess, A. (2007). A screen for nuclear transcripts identifies two linked noncoding RNAs associated with SC35 splicing domains. BMC Genomics *8*, 39.

Ji, P., Diederichs, S., Wang, W., Böing, S., Metzger, R., Schneider, P.M., Tidow, N., Brandt, B., Buerger, H., Bulk, E., et al. (2003). MALAT-1, a novel noncoding RNA, and thymosin beta4 predict metastasis and survival in early-stage non-small cell lung cancer. Oncogene *22*, 8031–8041.

Kapranov, P., Willingham, A.T., and Gingeras, T.R. (2007). Genome-wide transcription and the implications for genomic organization. Nature reviews *8*, 413–423.

Kato, L., Begum, N.A., Burroughs, A.M., Doi, T., Kawai, J., Daub, C.O., Kawaguchi, T., Matsuda, F., Hayashizaki, Y., and Honjo, T. (2012). Nonimmunoglobulin target loci of activation-induced cytidine deaminase (AID) share unique features with immunoglobulin genes. Proc. Natl. Acad. Sci. USA *109*, 2479–2484.

Khalil, A.M., Guttman, M., Huarte, M., Garber, M., Raj, A., Rivea Morales, D., Thomas, K., Presser, A., Bernstein, B.E., van Oudenaarden, A., et al. (2009). Many human large intergenic noncoding RNAs associate with chromatin-modifying complexes and affect gene expression. Proc. Natl. Acad. Sci. USA *106*, 11667–11672.

Lamond, A.I., and Spector, D.L. (2003). Nuclear speckles: a model for nuclear organelles. Nat. Rev. Mol. Cell Biol. *4*, 605–612.

Mao, Y.S., Sunwoo, H., Zhang, B., and Spector, D.L. (2011). Direct visualization of the co-transcriptional assembly of a nuclear body by noncoding RNAs. Nat. Cell Biol. *13*, 95–101.

Marahrens, Y., Panning, B., Dausman, J., Strauss, W., and Jaenisch, R. (1997). Xist-deficient mice are defective in dosage compensation but not spermatogenesis. Genes Dev. *11*, 156–166.

Martens, J.A., Laprade, L., and Winston, F. (2004). Intergenic transcription is required to repress the Saccharomyces cerevisiae SER3 gene. Nature *429*, 571–574.

Martianov, I., Choukrallah, M.A., Krebs, A., Ye, T., Legras, S., Rijkers, E., Van Ijcken, W., Jost, B., Sassone-Corsi, P., and Davidson, I. (2010). Cell-specific occupancy of an extended repertoire of CREM and CREB binding loci in male germ cells. BMC Genomics *11*, 530.

Mercer, T.R., Gerhardt, D.J., Dinger, M.E., Crawford, J., Trapnell, C., Jeddeloh, J.A., Mattick, J.S., and Rinn, J.L. (2012). Targeted RNA sequencing reveals the deep complexity of the human transcriptome. Nat. Biotechnol. *30*, 99–104.

Mohammad, F., Mondal, T., Guseva, N., Pandey, G.K., and Kanduri, C. (2010). Kcnq1ot1 noncoding RNA mediates transcriptional gene silencing by interacting with Dnmt1. Development *137*, 2493–2499.

Nakagawa, S., Naganuma, T., Shioi, G., and Hirose, T. (2011). Paraspeckles are subpopulation-specific nuclear bodies that are not essential in mice. J. Cell Biol. *193*, 31–39.

Ørom, U.A., Derrien, T., Beringer, M., Gumireddy, K., Gardini, A., Bussotti, G., Lai, F., Zytnicki, M., Notredame, C., Huang, Q., et al. (2010). Long noncoding RNAs with enhancer-like function in human cells. Cell *143*, 46–58.

Petruk, S., Sedkov, Y., Riley, K.M., Hodgson, J., Schweisguth, F., Hirose, S., Jaynes, J.B., Brock, H.W., and Mazo, A. (2006). Transcription of bxd noncoding RNAs promoted by trithorax represses Ubx in cis by transcriptional interference. Cell *127*, 1209–1221.

Rajaram, V., Knezevich, S., Bove, K.E., Perry, A., and Pfeifer, J.D. (2007). DNA sequence of the translocation breakpoints in undifferentiated embryonal sarcoma arising in mesenchymal hamartoma of the liver harboring the t(11;19)(q11;q13.4) translocation. Genes Chromosomes Cancer *46*, 508–513.

Rinn, J.L., Kertesz, M., Wang, J.K., Squazzo, S.L., Xu, X., Brugmann, S.A., Goodnough, L.H., Helms, J.A., Farnham, P.J., Segal, E., and Chang, H.Y. (2007). Functional demarcation of active and silent chromatin domains in human HOX loci by noncoding RNAs. Cell *129*, 1311–1323.

Robinson, M.D., McCarthy, D.J., and Smyth, G.K. (2010). edgeR: a Bioconductor package for differential expression analysis of digital gene expression data. Bioinformatics *26*, 139–140.

Sasaki, Y.T., Ideue, T., Sano, M., Mituyama, T., and Hirose, T. (2009). MENepsilon/beta noncoding RNAs are essential for structural integrity of nuclear paraspeckles. Proc. Natl. Acad. Sci. USA *106*, 2525–2530.

Schorderet, P., and Duboule, D. (2011). Structural and functional differences in the long non-coding RNA hotair in mouse and human. PLoS Genet. *7*, e1002071.

Shearwin, K.E., Callen, B.P., and Egan, J.B. (2005). Transcriptional interference—a crash course. Trends Genet. *21*, 339–345.

Sleutels, F., Zwart, R., and Barlow, D.P. (2002). The non-coding Air RNA is required for silencing autosomal imprinted genes. Nature *415*, 810–813.

Stadler, P. (2010). Evolution of the Long Non-coding RNAs MALAT1 and MENβ/ε. Advances in Bioinformatics and Computational Biology *6268*, 1–12.

Sunwoo, H., Dinger, M.E., Wilusz, J.E., Amaral, P.P., Mattick, J.S., and Spector, D.L. (2009). MEN epsilon/beta nuclear-retained non-coding RNAs are up-regulated upon muscle differentiation and are essential components of paraspeckles. Genome Res. *19*, 347–359.

Tripathi, V., Ellis, J.D., Shen, Z., Song, D.Y., Pan, Q., Watt, A.T., Freier, S.M., Bennett, C.F., Sharma, A., Bubulya, P.A., et al. (2010). The nuclear-retained noncoding RNA MALAT1 regulates alternative splicing by modulating SR splicing factor phosphorylation. Mol. Cell *39*, 925–938.

Tsai, M.C., Manor, O., Wan, Y., Mosammaparast, N., Wang, J.K., Lan, F., Shi, Y., Segal, E., and Chang, H.Y. (2010). Long noncoding RNA as modular scaffold of histone modification complexes. Science *329*, 689–693.

Turner, B.M., and Franchi, L. (1987). Identification of protein antigens associated with the nuclear matrix and with clusters of interchromatin granules in both interphase and mitotic cells. J. Cell Sci. *87*, 269–282.

Ulitsky, I., Shkumatava, A., Jan, C.H., Sive, H., and Bartel, D.P. (2011). Conserved function of lincRNAs in vertebrate embryonic development despite rapid sequence evolution. Cell *147*, 1537–1550.

Wilusz, J.E., Freier, S.M., and Spector, D.L. (2008). 3′ end processing of a long nuclear-retained noncoding RNA yields a tRNA-like cytoplasmic RNA. Cell *135*, 919–932.

Wilusz, J.E., Sunwoo, H., and Spector, D.L. (2009). Long noncoding RNAs: functional surprises from the RNA world. Genes Dev. *23*, 1494–1504.

Wilusz, J.E., Whipple, J.M., Phizicky, E.M., and Sharp, P.A. (2011). tRNAs marked with CCACCA are targeted for degradation. Science *334*, 817–821.

Yang, L., Lin, C., Liu, W., Zhang, J., Ohgi, K.A., Grinstein, J.D., Dorrestein, P.C., and Rosenfeld, M.G. (2011). ncRNA- and Pc2 methylation-dependent gene relocation between nuclear structures mediates gene activation programs. Cell *147*, 773–788.

Note Added in Proof

While our manuscript was in press, two additional studies describing similar phenotypes for the Malat1knockout mice came to our attention from the laboratories of Sven Diederichs (Eissmann et al., 2012) and Shinichi Nakagawa and Kannanganattu Prasanth (Nakagawa et al., 2012):

Eissmann, M., Gutschner, T., Hammerle, M., Gunther, S., Caudron-Herger, M., Gross, M., Schirmacher, P., Rippe, K., Braun, T., Zornig, M., et al. (2012). Loss of the abundant nuclear non-coding RNA MALAT1 is compatible with life and development. RNA Biol. 10.4161/rna.21089.

Nakagawa, S., Ip, J.Y., Shioi, G., Tripathi, V., Zong, X., Hirose, T. and K.V. Prasanth. (2012). Malat1 is not an essential component of nuclear speckles in mice. RNA. 10.1261/rna.033217.112.